Progress In Electromagnetics Research C, Vol. 134, 181–195, 2023

Identification of VNS-AGA Permanent Magnet Synchronous Wind Generator Parameters Considering Magnetic Saturation and VSI Compensation

Zhun Cheng[1], Chao Zhang[2], and Yang Zhang[2, *]

Abstract—In order to solve the problem of the influence of magnetic saturation and voltage source inverter (VSI) nonlinear factors on the parameter identification of permanent magnet synchronous wind generator (PMSWG), a variable neighborhood search-adaptive genetic algorithm (VNS-AGA) based on magnetic saturation and VSI compensation is proposed in this paper. Considering the existence of magnetic saturation, a mathematical model of PMSWG considering magnetic saturation is established. The least square method is used to identify the inductance of dq axis. The influence of VSI nonlinear factors on the system is regarded as a disturbance voltage, which is used as an electrical parameter; the parameters of PMSWG are identified simultaneously; and voltage compensation is carried out. After the accurate distortion voltage compensation mathematical model and fitness function are established, GA and adaptive algorithm are combined to increase the diversity of the population. Then variable neighborhood search (VNS) strategy is introduced to search the optimal region. Experimental results show that the proposed method is more accurate and convergent after considering magnetic saturation and on-line identification and compensation of disturbance voltage.

1. INTRODUCTION

Wind power generation as a renewable energy generation method has been developing rapidly in recent years [1]. With the development of power electronics and advanced control methods, PMSWG has gradually become the mainstream of wind power generation at this stage [2, 3]. The accuracy of the PMSWG high performance control system is related to the motor parameters, which are generally the standard minimum values and do not take into account the parameter changes of the motor at the moment of operation. When the PMSWG is in operation, the parameters will change with the change in temperature. The stator resistance and the permeability of the ferromagnet have a nonlinear relationship with the temperature, which leads to a mismatch between the proportional-integral (PI) controller parameters and the actual parameters of the PMSWG and reduces the dynamic and steady-state performance of the PMSWG. The determination of these parameters mainly depends on the accuracy of PMSWG parameters; therefore, accurate identification of PMSWG parameters is the key to improving the performance of the PMSWG drive system [4–6]. There are two main methods for PMSWG parameter identification, namely, offline identification method and online identification method.

In offline identification, the identification method generally involves obtaining the motor parameters by injecting a certain frequency and amplitude voltage with the motor stationary or slightly moving. Although offline identification can provide initial values for PI controller design, ignoring eddy current losses in the motor core and possible parameter variations caused by permanent magnet temperature

Received 10 May 2023, Accepted 14 June 2023, Scheduled 9 July 2023
* Corresponding author: Yang Zhang (459387623@qq.com).
[1] Hunan Railway Professional Technology College, Zhuzhou 412001, China. [2] Hunan University of Technology, Zhuzhou 412007, China.

makes offline parameter identification methods unable to track online [7–9]. Online identification can automatically correct PI controller parameters through real-time parameter measurement with motor operation data, which can effectively solve the problem of system control performance degradation caused by parameter changes [10]. The traditional methods for online identification are least squares (LS), extended Kalman filter (EKF), and model reference adaptive system (MRAS); however, with the increasingly complex operating conditions of PMSWG and the strong coupling of motor parameters, the traditional methods cannot meet the requirements of online identification. Reference [11] proposed a recursive least squares (RLS) method for parameter identification based on LS, analyzed the factors affecting the identification accuracy, and the identification results can be close to the actual values, but the increase in the amount of data leads to data saturation, which makes the identification accuracy decrease. Reference [12], the optimized EKF was used to measure the motor parameters, and the method is less computational, but the system noise matrix Q and measurement matrix R require a large number of experiments to obtain them, which is difficult to implement in practical applications. Reference [13] designed the adaptive rates of resistance, inductance, and magnetic chain of the motor, respectively, and although the recognition in effect is good, the design of adaptive rates is a difficult point in the implementation of the MRAS recognition system, and there is the problem of scattering of recognition results due to multi-parameter recognition in the case of under-ranking. With the development of technology, the computing power of computers has been greatly improved, and intelligent algorithms have been developed in parameter identification and optimization with the help of computer technology [14, 15]. Intelligent algorithms do not require initial values of parameters, have the advantages of fast speed and low cost, and are widely used in motor parameter identification [16]. The common intelligent algorithms are artificial neural networks (ANN), genetic algorithms (GA), and particle swarm algorithms (PSO). References [17, 18] used neural network algorithms for motor parameter identification and analyzed the effect of neural network learning rate on parameter identification, although the accuracy of parameter identification is high. The initial values require a lot of training, which makes the neural network algorithm design more complex. Reference [19] introduced the relevant concepts of quantum mechanics into the particle evolution process and proposed the quantum particle swarm algorithm, which discarded the speed term of the particle swarm algorithm to obtain a faster convergence rate and overcame the limitation that the parameters of the particle swarm algorithm were difficult to determine, but the problem of convergence to a local optimum was still unavoidable.

GA is widely used in the field of parameter identification for its wide applicability, good stability, and robustness. In [20], GA was used to identify the parameters of electric machines, and it was shown experimentally that the method had high accuracy, but it was computationally intensive and prone to local optimum problems. In [21], quantum rotational gates and multi-state quantum bit encoding operations were added to the GA, and it was experimentally shown that the method had a high parametric search capability and was fast, but there were problems of under-ranking and high complexity.

When PMSWG is in actual operation, it will be inevitably affected by the nonlinear factors of VSI, which mainly include the switching distortion of switching devices, the nonlinearity of inductors and capacitors, and the noise of the power supply [22]. The disturbance voltage generated by VSI nonlinear factors will distort inverter output voltage and current, resulting in motor output torque fluctuation, noise increase, efficiency reduction, and other problems [23]. Reference [24] proposed an online estimation method of rotor flux and VSI nonlinearity of permanent magnet synchronous motor driver, and an online estimation of distortion voltage caused by VSI nonlinearity was used to estimate rotor flux. Reference [25] took into account the nonlinear effects of VSI in the parameter estimation model, and distortion voltage can be estimated simultaneously with other motor parameters, which can effectively track machine parameter variations by compensating for nonlinear factors.

In PMSWG, magnetic saturation occurs when the magnetic flux density in the solenoid coil reaches a certain value, leading to a decrease in the permeability of the coil, resulting in a decrease in the output power and efficiency of the motor. When performing motor parameter identification, considering the effect of magnetic saturation on the motor can provide more accurate motor parameters, thus improving the accuracy and efficiency of motor control. In [26], a torque pulsation suppression method with online identification of dq-axis inductance parameters with magnetic saturation was proposed, and the

identified parameters were used to achieve accurate torque control of a permanent magnet synchronous motor. In [27], a space vector dynamics model identification method for a rotating induction motor model considering both magnetic saturation and iron losses was proposed by modeling the magnetic saturation effect and subsequently estimating the electrical parameters of this model using the genetic algorithm offline technique, which experimentally showed a higher accuracy of electrical parameter identification.

In this paper, the mathematical model of the ideal PMSWG is changed by practical situations, taking into account the influence of the nonlinear factors of the power-type inverter on the parameter identification and the effect of the magnetic saturation effect of the motor on the inductance. The work of our paper is summarized as follows:

(1) Considering the existence of magnetic saturation, which leads to the nonlinear variation of the inductance of PMSWG, the second-order polynomial is used to fit the relationship between inductance and current, and the dq-axis inductance is identified by the least-squares method, which improves the accuracy of VNS-AGA method identification in combination with the nonlinear model of PMSWG.

(2) To solve the influence of VSI nonlinear factors on the operating performance of PMSWG, a mathematical model of nonlinear factors is established? The influence of nonlinear factors on the system is regarded as a disturbance voltage to be identified, and the disturbance voltage identified by the VNS-AGA method is corrected in real-time to obtain higher identification accuracy.

(3) The VNS strategy is introduced in the AGA to make the parameter identification results more accurate by discovering more potential optimal solution regions in the search space and performing a fine search in the current optimal solution region.

2. MATHEMATICAL MODEL OF PMSWG

2.1. The Ideal Model of PMSWG

In the process of parameter identification, the reference voltage output by the PI current controller will be used instead of the measured voltage; however, the actual voltage applied to the phase winding is not equal to the voltage output by the PI current controller due to the existence of the VSI nonlinear factor, and the VSI nonlinear factor must be considered in the identification model to improve the accuracy of identification.

$$\begin{cases} u_D = u_d + V_{d\text{-}dis} \\ u_Q = u_d + V_{q\text{-}dis} \end{cases} \tag{1}$$

$$\begin{cases} V_{d\text{-}dis} = D_d V_{dis} \\ V_{q\text{-}dis} = D_q V_{dis} \end{cases} \tag{2}$$

where D_d and D_q are the dq-axis periodic perturbation components, respectively; V_{dis} is the effect of the VSI nonlinear factor on the system viewed as a perturbation voltage.

$$\begin{cases} u_D = Ri_d - \omega L_q i_q + D_d V_{dis} \\ u_Q = Ri_q - \omega L_d i_d + \omega\varphi_f + D_q V_{dis} \end{cases} \tag{3}$$

$$\begin{bmatrix} D_d \\ D_q \end{bmatrix} = \frac{1}{3} \begin{bmatrix} \cos\theta & \sin\theta \\ -\sin\theta & \cos\theta \end{bmatrix} \begin{bmatrix} 1 & -\frac{1}{2} & -\frac{1}{2} \\ 0 & \frac{\sqrt{3}}{2} & -\frac{\sqrt{3}}{2} \end{bmatrix} \begin{bmatrix} \text{sign}(i_A) \\ \text{sign}(i_B) \\ \text{sign}(i_C) \end{bmatrix} \tag{4}$$

where i_A is the three-phase current of stator ABC.

The principle of parameter identification is shown in Fig. 1.

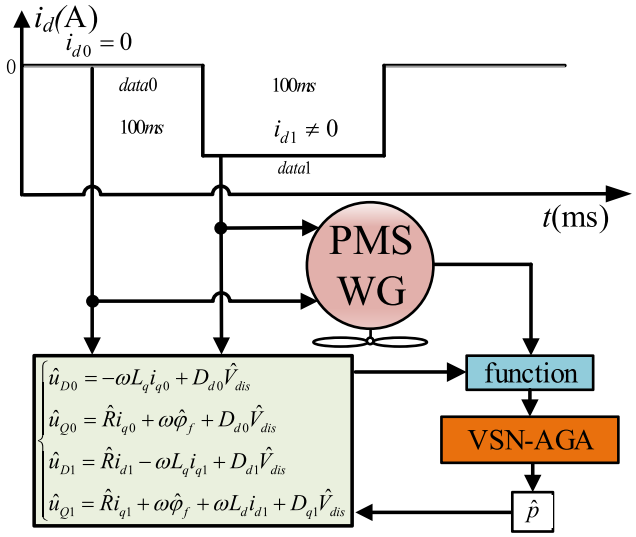

Figure 1. Block diagram of the identification principle.

2.2. Fitness Function Design for VSI Nonlinear Factors

Vector control methods are adopted in this paper, as shown in Equation (5).

$$\begin{cases} \hat{u}_{D0}(k) = -\omega(k) L_q i_{q0}(k) + D_{d0}(k)\hat{V}_{dis} \\ \hat{u}_{Q0}(k) = \hat{R}i_{q0}(k) + \omega(k)\hat{\varphi}_f + D_{d0}(k)\hat{V}_{dis} \\ \hat{u}_{D1}(k) = \hat{R}i_{d1}(k) - \omega(k) L_q i_{q1}(k) + D_{d1}(k)\hat{V}_{dis} \\ \hat{u}_{Q1}(k) = \hat{R}i_{q1}(k) + \omega(k)\hat{\varphi}_f + \omega(k) L_d i_{d1}(k) + D_{q1}(k)\hat{V}_{dis} \end{cases} \tag{5}$$

where $\hat{u}_{D0}(k)$, $D_{d0}(k)$ are the data sampled at the Kth time; $\hat{u}_{D1}(k)$, $\hat{u}_{Q1}(k)$, $i_{d1}(k)$, $i_{q1}(k)$, $D_{d1}(k)$, $D_{q1}(k)$ are the data sampled at the Kth time.

$$\begin{cases} p_1\left(\hat{R}, \hat{\varphi}_f, \hat{V}_{dis}\right) = \dfrac{1}{W}\left[u_{Q0}(k) - \hat{u}_{Q0}(k)\right]^2 \\ p_2\left(\hat{R}, \hat{V}_{dis}\right) = \dfrac{1}{W}\left[u_{D1}(k) - \hat{u}_{D1}(k)\right]^2 \\ p_3\left(\hat{R}, \hat{\varphi}_f, \hat{V}_{dis}\right) = \dfrac{1}{W}\left[u_{Q1}(k) - \hat{u}_{Q1}(k)\right]^2 \end{cases} \tag{6}$$

where W is the maximum number of iterations.

The fitness function is shown in Equation (7).

$$P_{\min} = \sum_{i=1}^{3} w_i p_i \tag{7}$$

where w_i is the weighting coefficient. Since the identification parameters are all important, the weighting coefficient is taken as 1/3.

2.3. Magnetic Saturation Model of PMSWG

Due to the existence of the magnetic saturation effect, PMSWG quadrature axis inductance is difficult to measure, so the second-order polynomial is used to fit the relationship between inductance and current, as shown in the following equation.

$$\begin{cases} L_{d1}(i_{d1}, i_{q1}) = L_{d0} + m_1 i_{d1} + m_2 i_{q1} + m_3 i_{d1}^2 + m_4 i_{q1}^2 + m_5 i_{d1} i_{q1} \\ L_{q1}(i_{d1}, i_{q1}) = L_{q0} + n_1 i_{d1} + n_2 i_{q1} + n_3 i_{d1}^2 + n_4 i_{q1}^2 + n_5 i_{d1} i_{q1} \end{cases} \tag{8}$$

where L_{d0} is a constant; m_1, m_3, n_1, n_3 are the self-saturation effect coefficients of dq axis inductance, respectively. m_2, m_4, n_2, n_4 are the cross saturation coefficients of dq axis inductors, respectively.

By substituting Equation (8) into Equation (3)

$$\begin{cases} u_D = Ri_{d1} - \omega L_{q1}\left(i_{d1}, i_{q1}\right) i_{q1} + D_d V_{dis} \\ u_Q = Ri_{q1} - \omega L_{d1}\left(i_{d1}, i_{q1}\right) i_{q1} i_{d1} + \omega\varphi_f + D_q V_{dis} \end{cases} \tag{9}$$

3. PMSWG PARAMETER IDENTIFICATION METHOD

3.1. Inductance Identification Considering Magnetic Saturation

Due to magnetic saturation, the inductance of the motor will change nonlinearly with the current of the stator. To improve the identification performance, the unary quadratic equation given in Equation (8) is used to fit the relationship between inductance and current. For parameter identification, to accurately identify motor parameters from a large number of data, two variables y_1, y_2 unrelated to speed will be defined. First, the least square method will be used to identify the two variables, and then the parameters will be identified from these variables.

$$\begin{cases} x_1 = Ri_{d1} + D_d V_{dis} \\ x_2 = Ri_{q1} + D_q V_{dis} \\ y_1 = \left(L_{d0} + m_1 i_{d1} + m_2 i_{q1} + m_3 i_{d1}^2 + m_4 i_{q1}^2 + m_5 i_{d1} i_{q1}\right) i_{q1} \\ y_2 = \left(L_{q0} + n_1 i_{d1} + n_2 i_{q1} + n_3 i_{d1}^2 + n_4 i_{q1}^2 + n_5 i_{d1} i_{q1}\right) i_{d1} + \varphi_f \end{cases} \tag{10}$$

So, Equations (4)–(8) can be expressed as

$$\begin{cases} u_D = x_1 - \omega y_1 \\ u_Q = x_2 - \omega y_2 \end{cases} \tag{11}$$

Given the current of the dq axis i_{d1} and i_{q1}, the measured voltage is collected at N different speeds, expressed as $\omega_1, \cdots, \omega_n$, and the measured voltage can be expressed as $u_{D1,n}, u_{Q1,n}$, $n = 1, \cdots, N$. Equation (11) can be expressed as (12).

$$\begin{cases} u_{D1,n} = x_1 - \omega_n y_1 \\ u_{Q1,n} = x_2 - \omega_n y_2 \end{cases} \tag{12}$$

$u_{D1,n}$ and $u_{Q1,n}$ are collected at the rate of ω_n, of which x_1, x_2, y_1, y_2 can be identified using the least square method in Equations (14) and (17).

Given $y_{1,k}$, $k = 1, ..., K$, Equation (10) gives (13).

$$y_{1,k} = \left(L_{d0} + m_1 i_{d1} + m_2 i_{q1} + m_3 i_{d1}^2 + m_4 i_{q1}^2 + m_5 i_{d1} i_{q1}\right) i_{q1,k}, \quad k = 1, \cdots, K \tag{13}$$

$$X_{L_d} = \left(\Phi_{L_d}^T \Phi_{L_d}\right)^{-1} \Phi_{L_d}^T Y_{L_d} \tag{14}$$

$$X_{L_d} = \begin{bmatrix} L_{d0} \\ m_1 \\ m_2 \\ m_3 \\ m_4 \\ m_5 \end{bmatrix}, \; Y_{L_d} = \begin{bmatrix} L_{d1} \\ \vdots \\ L_{dn} \end{bmatrix}, \; \Phi_{L_d} = \begin{bmatrix} i_{q1,1} & i_{d1,1} i_{q1,1} & i_{q1,1}^2 & i_{q1,1} i_{d1,1}^2 & i_{q1,1}^3 & i_{d1,1} i_{q1,1}^2 \\ & & \vdots & & & \\ i_{q1,K} & i_{d1,K} i_{q1,K} & i_{q1,K}^2 & i_{q1,K} i_{d1,K}^2 & i_{q1,K}^3 & i_{d1,K} i_{q1,K}^2 \end{bmatrix} \tag{15}$$

According to Equation (15), $L_{d0}, m_1, m_2, m_3, m_4, m_5$ can be identified.

Equation (10) can be used to obtain (16).

$$y_{2,k} = \left(L_{q0} + n_1 i_{d1} + n_2 i_{q1} + n_3 i_{d1}^2 + n_4 i_{q1}^2 + n_5 i_{d1} i_{q1}\right) i_{d1,k} + \varphi_f \tag{16}$$

$$X_{L_q} = \left(\Phi_{L_q}^T \Phi_{L_q}\right)^{-1} \Phi_{L_q}^T Y_{L_q} \tag{17}$$

$$X_{L_q}=\begin{bmatrix} L_{q0} \\ n_1 \\ n_2 \\ n_3 \\ n_4 \\ n_5 \end{bmatrix},\ Y_{L_q}=\begin{bmatrix} L_{q1} \\ \vdots \\ L_{qn} \end{bmatrix},\ \Phi_{L_q}=\begin{bmatrix} i_{d1,1} & i_{d1,1}^2 & i_{d1,1}i_{q1,1} & i_{d1,1}^3 & i_{d1,1}i_{q1,1}^2 & i_{d1,1}^2 i_{q1,1} \\ & & \vdots & & & \\ i_{d1,K} & i_{d1,K}^2 & i_{d1,K}i_{q1,K} & i_{d1,K}^3 & i_{d1,K}i_{q1,K}^2 & i_{d1,K}^2 i_{q1,K} \end{bmatrix}+\varphi_f \tag{18}$$

According to Equation (18), $L_{q0}, n_1, n_2, n_3, n_4, n_5$ can be identified.

In order to identify the above parameters, $K > 6$. $L_{d0}, m_1, m_2, m_3, m_4, m_5$ and $L_{q0}, n_1, n_2, n_3, n_4, n_5$ can be identified according to Equations (15) and (18), and L_{d1} and L_{q1} can be identified according to Equation (8).

If the decoupling scheme is not employed, one needs to estimate multi-parameters simultaneously from all the measurements, in which the estimation error of one parameter could affect the estimation accuracy of other parameters. Experimental data collection of PMSWG inductance identification is shown in Fig. 2.

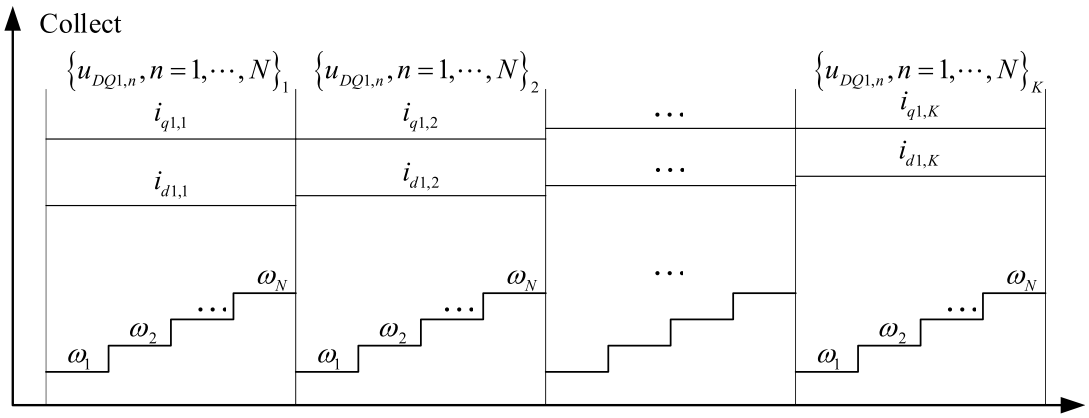

Figure 2. Experimental data collection of PMSWG inductance identification.

3.2. Adaptive Genetic Algorithm

The crossover rate and mutation rate are kept constant during the evolution of GA. During the initialization of the population, the diversity of the population is high, and the crossover rate and mutation rate at this time do not have much effect on the population. However, in the evolutionary stage of the population, the better individuals need smaller crossover rates and mutation rates, and the opposite for the worse individuals, so the constant crossover rates and mutation rates adversely affect the diversity of the population and the convergence of the algorithm. With AGA, the crossover rate and mutation rate are made to vary with the fitness value of the population. The crossover rate and mutation rate of AGA are calculated as follows:

$$P_c = \begin{cases} \dfrac{k_1 (f_{\max} - f')}{f_{\max} - f_{\min}}, & f' \geq f_{avg} \\ k_2, & f' < f_{avg} \end{cases} \tag{19}$$

$$P_m = \begin{cases} \dfrac{k_3 (f_{\max} - f_{avg})}{f_{\max} - f_{\min}}, & f \geq f_{avg} \\ k_4, & f < f_{avg} \end{cases} \tag{20}$$

where $f_{\max}$ is the maximum fitness value among population individuals, $f_{\min}$ the minimum fitness value among population individuals, f_{avg} the mean value among population individuals, f' the maximum fitness value between two individuals in the crossover operation, f the fitness value in the variation operation, and k_1, k_2, k_3, k_4 are the random numbers between [0 1].

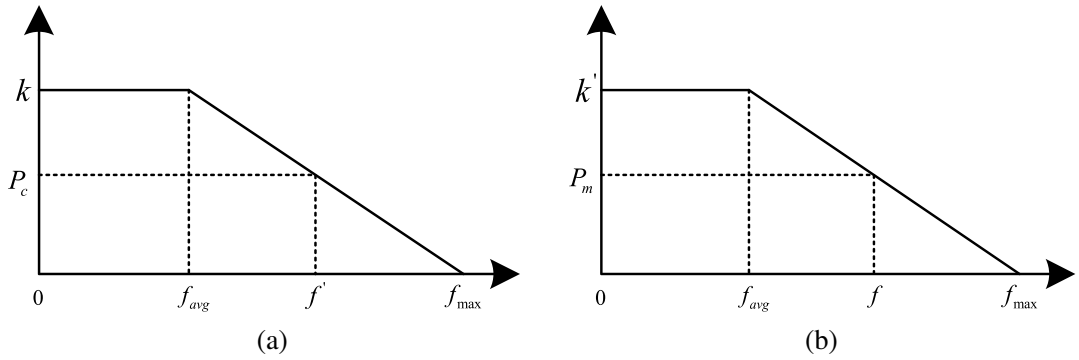

Figure 3. Diagram general description. (a) Crossover rate adjustment curve; (b) mutation rate adjustment curve.

From Fig. 3, when the fitness of the population is smaller than the average fitness of the individuals, the crossover rate and variation rate remain constant, and when the fitness of the population is between the average fitness and the maximum fitness of the individuals, the population fitness is linearly related to the crossover rate and variation rate. This also indicates that when the fitness value of the population is small, a larger crossover rate and variation rate are needed to make the individuals evolve better; the larger the fitness value of the individuals is, the smaller the crossover rate and variation rate are, which also indicates that the better individuals do not need to evolve and keep the most individuals.

3.3. Variable Neighborhood Search Strategy

The idea of variable neighborhood search (VNS) is to systematically change the volume neighborhood structure set in the search process to expand the search range and obtain a local optimal solution, and then systematically change the volume neighborhood structure set again based on this local optimal solution to expand the search range and find another local optimal solution.

The steps of the VNS strategy are as follows:

(1) Initial value x, defining the set of variable neighborhood structures $N_i(x)$, $i = 1$ as the starting point of the search.

(2) The variable neighborhood structure set is used to search, and the current optimal solution is disturbed or transformed. If a better solution $N_k(x)$ than x is found in x', then $x = x'$, $i = 1$.

(3) If the variable neighborhood search set still cannot find a better solution than x, let i++.

(4) Compare the current optimal solution with the historical optimal solution. If the current optimal solution is better, update the historical optimal solution; otherwise, go back to step (1) and redefine the neighborhood structure.

(5) Repeat the above steps until the stop criterion is met, and x is printed.

(6) The variable neighborhood search strategy is combined with adaptive genetic algorithm, and the local search ability of variable neighborhood search and the global search ability of adaptive genetic algorithm are used to find high quality solutions quickly.

The steps of VNS-AGA are as follows:

(1) Let the initial solution be x, the set of variable neighborhood structures $N_k(x)$, $k = 1, 2, ..., k_{\max}$, the initial values of the parameters $k_{\max}$, $t_{\max}$, k_{step}, where $k_{\max}$ is the maximum domain, $t_{\max}$ the maximum computation time, and k_{step} the number of domain steps per iteration.

(2) Search for a local optimal solution in the neighborhood of the current solution. If a better local optimal solution is found, the neighborhood change is carried out.

(3) Randomly generate $x'_1, x'_2, ..., x'_r$ $(x'_1, x'_2, ..., x'_r \in N_p(x))$ in the pth domain structure set of x.

(4) Run AGA to obtain the local optimal solution $x'_1, x'_2, ..., x'_r$, and choose $x'_1, x'_2, ..., x'_r$ the best as x'' , i.e., $f(x'') = \min\limits_{1 \le i \le r} f(x'')$.

(5) If $f(x'') = \min\limits_{1\le i\le r} f(x'')$, $x = x'$, go to step (1); conversely, make $k = k + k_{\text{step}}$ and go to step (2).

(6) Repeat the above steps until the stopping criterion is met.

The flowchart of VNS-AGA to identify PMSWG parameters is shown in Fig. 4.

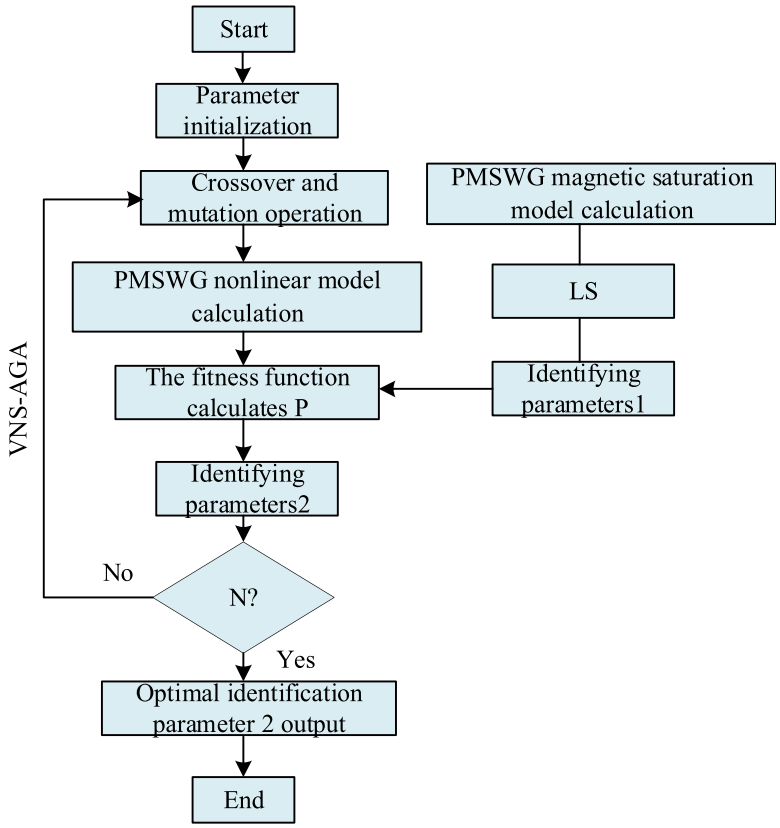

Figure 4. Flowchart of VNS-AGA identification of PMSWG parameters.

4. EXPERIMENTAL RESULTS AND ANALYSIS

Figure 5 is block diagram of the vector control strategy with $id = 0$, and the RT-LAB hardware-in-the-loop simulation (HILS) experiment platform is shown in Fig. 6, which is used to verify the feasibility of the proposed method. The digital signal processing (DSP) controller running the algorithm is TMS320F2812. The parameters of PMSWG and power device are shown in Table 1.

The proposed identification method VNA-AGA is compared with AGA and hybrid genetic algorithm (HGA) [28]. The three methods can identify and compensate the disturbance voltage. The parameters of these methods are set as follows: population size is 20; crossover rate is 0.75; mutation rate is 1.5; running time is 0.5 s; iteration time is the ratio of running time to sampling time; and system sampling frequency is 10 kHz. In order to make the identification results clear observation, the resistance, flux, and disturbance voltage are expanded by 10, 5, and 100 times, respectively.

The identification results and errors are shown in Table 2.

The identification curves of Ld and Lq are shown in Fig. 7. Considering the existence of magnetic saturation, the actual value of Ld is 5.2 mH, and the identification result is 5.28 mH, which is 0.08 mH different from the actual value; the actual value of Lq is 11.5 mH, and the identification result is 11.82 mH, with an error of 2.8%. The identification curve of magnetic flux is shown in Fig. 8. The actual value of magnetic flux in the offline state of the motor in this paper is 0.175 Wb, and the identification result of the proposed VNS-AGA method is 0.178 Wb, which is different from the actual value by 0.003 Wb, with an error of 1.9%. In addition, the errors of the identification results of AGA

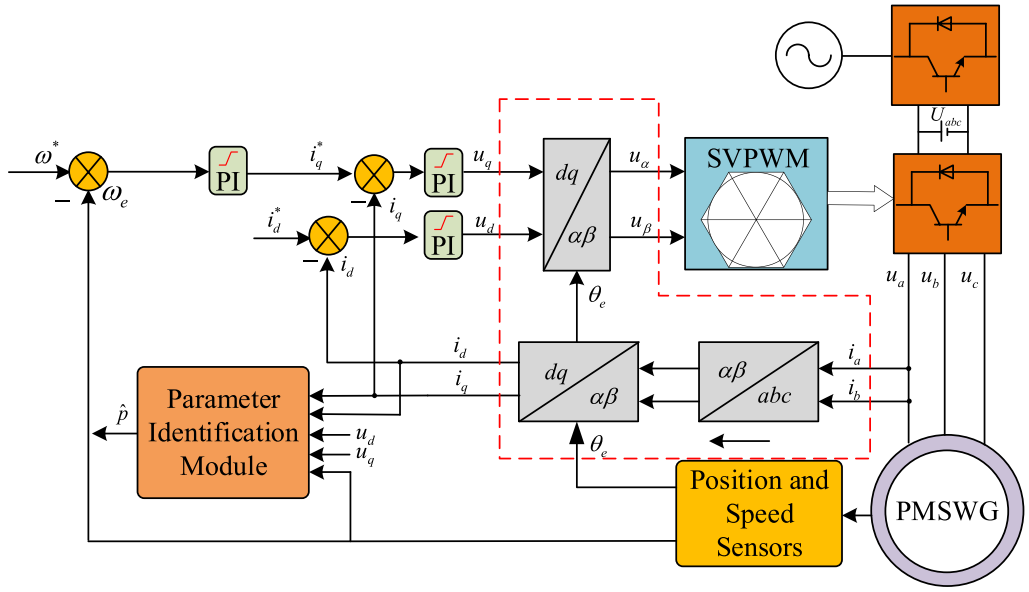

Figure 5. Conceptual diagram of vector control strategy with $i_d = 0$.

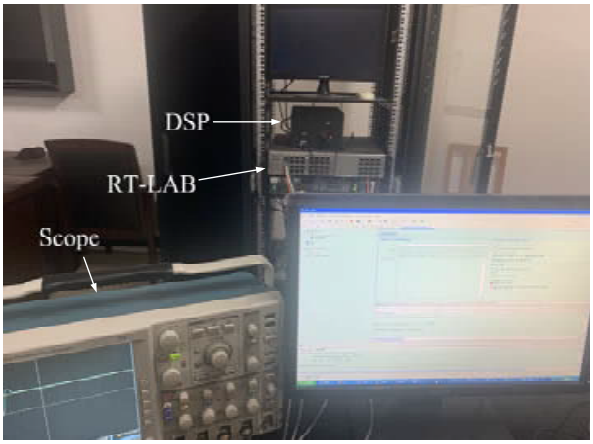

Figure 6. RT-LAB experimental platform.

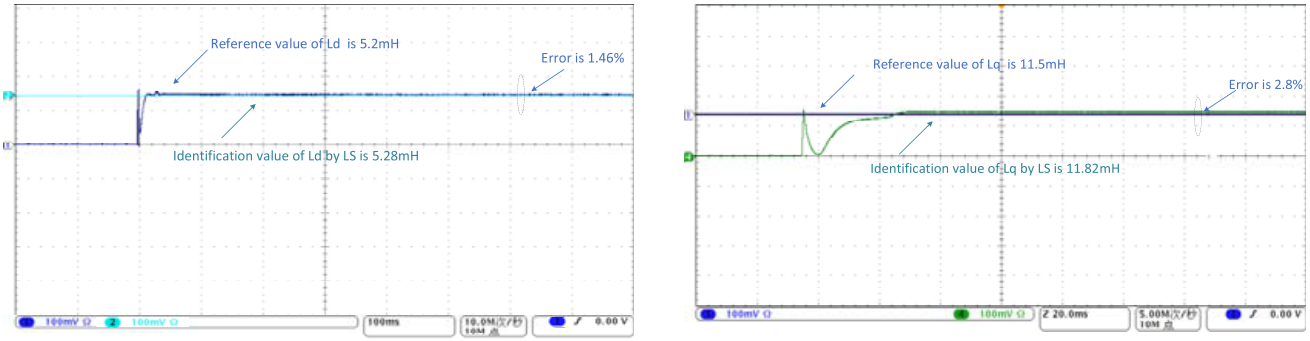

Ld *Lq*

Figure 7. *Ld* and *Lq* identification curve.

Table 1. PMSWG parameter.

Parameters	Value
Polar number	4
Stator resistance/Ω	0.933
Stator d axis inductance/mH	5.20
Stator q axis inductance/mH	11.5
Permanent magnet flux/Wb	0.175
Torque inertia/kg·m^2	0.003
Rated voltage/V	380
Rated torque/(N·m^2)	10
Rated speed/(r/min)	1000
Coefficient of viscous friction B/N·m/rad/s	0.1

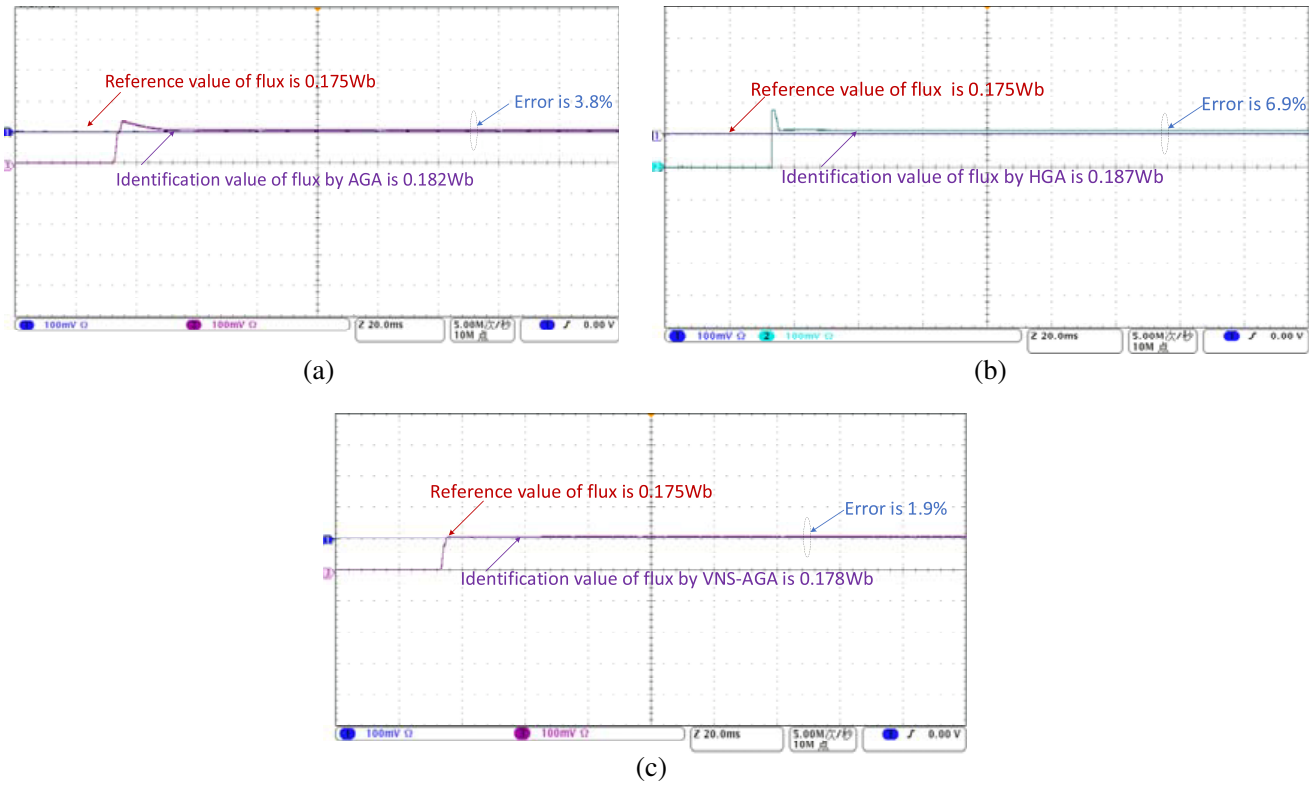

Figure 8. Permanent magnet flux identification curve. (a) AGA, (b) HGA, (c) VNS-AGA.

and HGA proposed in the paper are 3.8% and 6.9% from the actual values, and the errors of the AGA and HGA methods are 2 and 3.6 times of the errors of the proposed VNS-AGA method, respectively.

Figures 9 and 10 show the graphs of resistance and disturbance voltage under the three identification methods, respectively, and the errors of the resistance and disturbance voltage identification results are similar. As shown in Fig. 9, the result of resistance identification under optimization VNS-AGA is 1.898 Ω, and the error of the result with the actual value of motor resistance is 1.82%; the errors of the result with the actual value under two algorithms of AGA and HGA are 5.31% and 2.9%, respectively,

Table 2. Comparison of three algorithms simulation.

Parameters	AGA	HGA	VNS-AGA
Stator resistance/Ω	0.982	0.960	0.949
error/%	5.31	2.90	1.82
V_{dis}/V	0.962	−1.027	−1.019
error/%	3.8	−2.6	−1.9
Permanent magnet flux/Wb	0.182	0.187	0.178
error/%	3.8	6.9	1.9
Identification time/ms	67	42	31
Fitness value	0.935	0.721	0.614

and the error of the AGA identification result is 2.9 times of the error of the VNS-AGA identification result. As shown in Fig. 10, the discrimination result of the disturbance voltage under the optimized VNS-AGA is −1.019 V; the error of the result with the actual value of the disturbance voltage is 1.9%; the discrimination result of the AGA is −1.072 V; and the discrimination error is 7.2%, which is 3.8 times of the discrimination error of the VNS-AGA. The self-adaptive process does not find that the corresponding crossover rate is too small, which will lead to stagnant search and make the discrimination voltage converge locally with large error.

Through the experimental analysis, the error between the results of AGA and VNS-AGA identification and the actual values are different, which further indicates that by adding the variable neighborhood strategy, the initial population is more evenly distributed; the diversity of the population is better preserved; and the current optimal interval is searched more accurately, which makes the identification results more accurate. In the comparison of the three algorithms, the error of AGA is the largest, and the error of VNS-AGA is the smallest in the identification results of resistance and perturbation voltage; the error of HGA is the largest, and the error of VNS-AGA is the smallest in the identification results of magnetic flux.

The fitness function curves of the three algorithms in this paper are shown in Fig. 11. By the VNS-AGA discrimination method, it converges to 0.614 at 31 ms, and the final fitness values of the AGA and HGA discrimination methods are 0.935 and 0.721, respectively. The convergence times are 67 ms and 42 ms, respectively, and among the three algorithms, VNS-AGA has the smallest fitness and converges the fastest, so it can be concluded that the convergence of the identification results is faster by adding the variable neighborhood strategy.

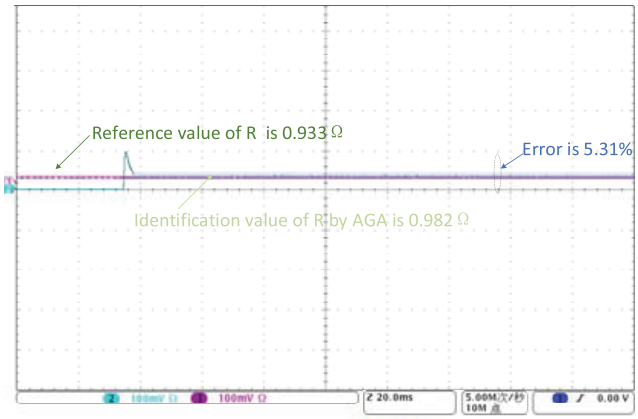

(a)

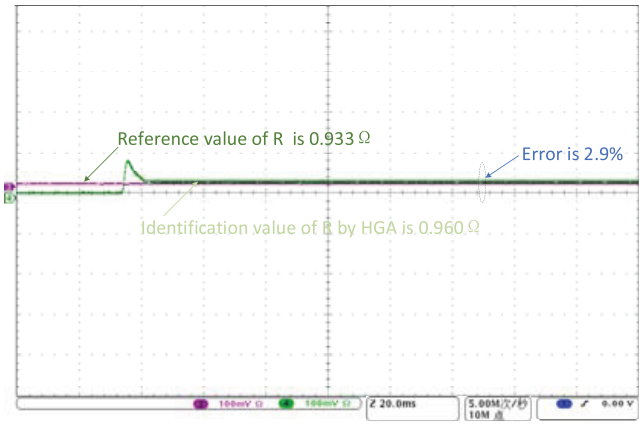

(b)

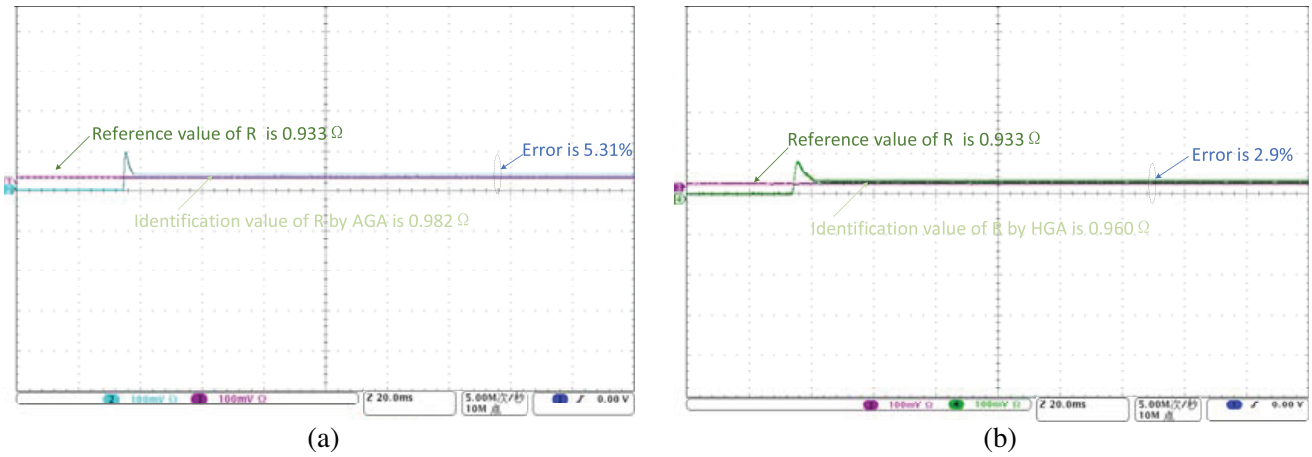

(a) (b)

Figure 9. Stator resistance identification curve. (a) AGA, (b) HGA, (c) VNS-AGA.

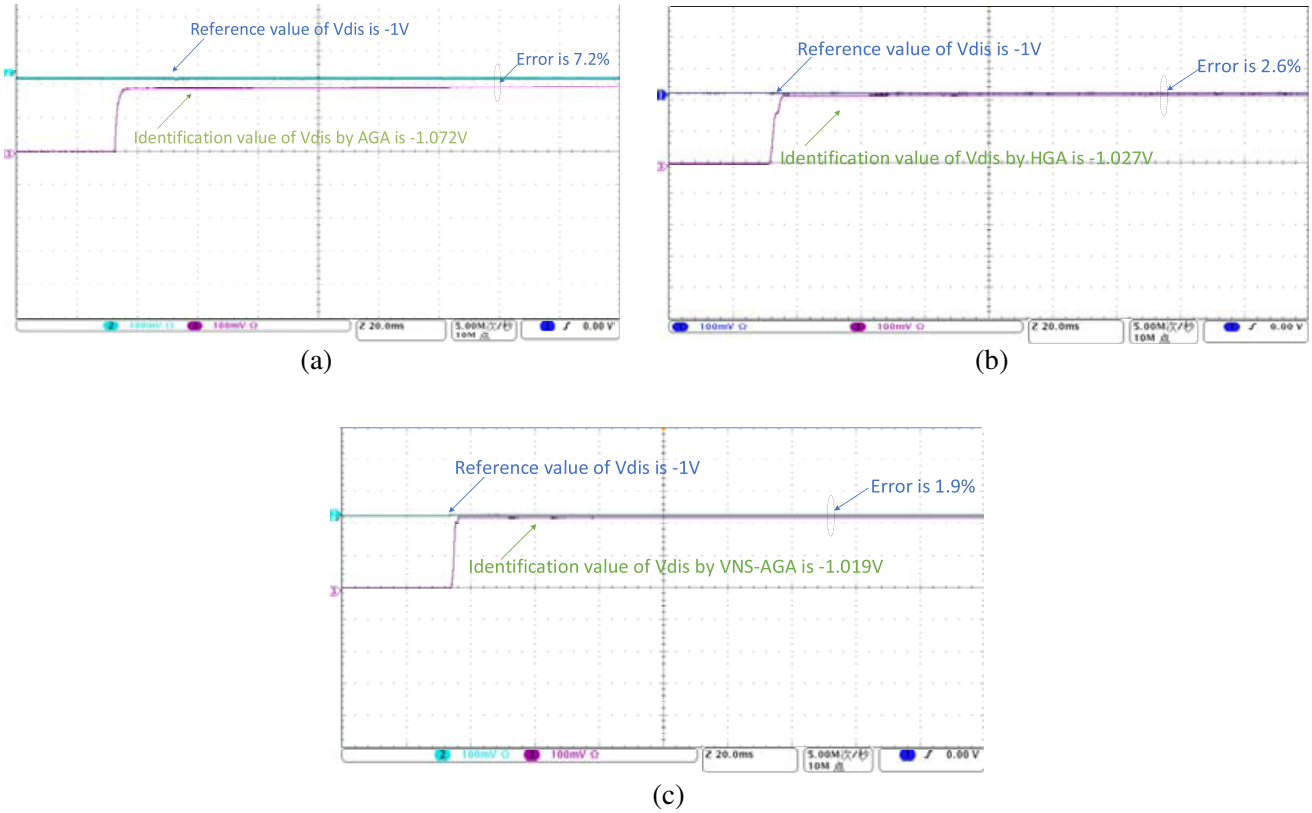

(a) (b)

(c)

Figure 10. Disturbance voltage identification curve. (a) AGA, (b) HGA, (c) VNS-AGA.

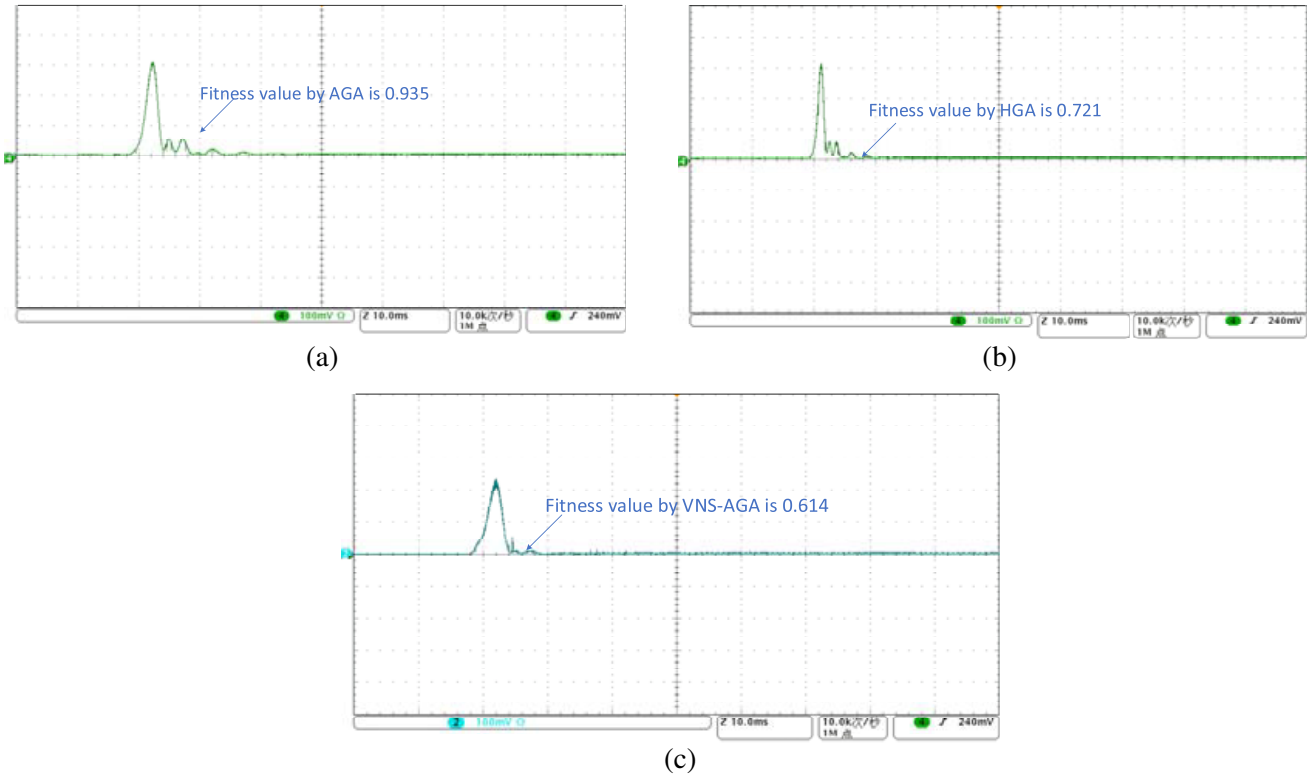

Figure 11. Fitness function value curve. (a) AGA, (b) HGA, (c) VNS-AGA.

5. CONCLUSION

Due to the influence of magnetic saturation and VSI nonlinear factors, the precision error of PMSWG identification increases, and the convergence rate slows down. A method of PMSWG parameter identification with VNS-AGA considering magnetic saturation and VSI compensation is proposed. Considering the existence of magnetic saturation, a mathematical model of PMSWG considering magnetic saturation is established. The least square method is used to identify the inductance of dq axis. The influence of VSI nonlinear factors on the system is regarded as a disturbance voltage, which is used as an electrical parameter. The parameters of PMSWG are identified simultaneously, and voltage compensation is carried out. A variable neighborhood search strategy is introduced in the AGA for a fine search of the current optimal region. Conclusions from the experiments are:

(1) The least square method is used to identify the inductance of dq axis, and the stator resistance, permanent magnet flux, and disturbance voltage can be identified by using the identified dq inductance and the proposed VNS-AGA method.

(2) After considering magnetic saturation and VSI compensation, the accuracy error of VNS-AGA identification method is 1%–2%, and the convergence time is 31 ms, which is more accurate and faster than AGA and HGA.

ACKNOWLEDGMENT

This work was supported by the Natural Science Foundation of Hunan Province of China under Grant Number 2022JJ50094.

REFERENCES

1. Zhang, Y. and S. Ula, "Comparison and evaluation of three main types of wind turbines," *2008 IEEE/PES Transmission and Distribution Conference and Exposition*, 1–6, IEEE, 2008.
2. Shen, Y. W., J. Zhang, Y. Y. Chen, A. Pi, and T. Cui, "Electromagnetic transient model and parameters identification of PMSG-based wind farm," *2019 IEEE 3rd Conference on Energy Internet and Energy System Integration (EI2)*, 72–77, IEEE, 2019.
3. Liu, J., H. Nian, J. Li, et al., "Sensorless control of PMSG for wind turbines based on the on-line parameter identification," *International Conference on Electrical Machines and Systems*, 1–6, IEEE, 2009.
4. Huy Anh, H. P., P. Quoc Khanh, and C. Van Kien, "Advanced PMSM machine parameter identification using modified jaya algorithm," *2019 International Conference on System Science and Engineering (ICSSE)*, 445–450, 2019.
5. Liu, H., S. Chen, and C. Hui, "The parameters identification of PMSM based on model reference adaptive," *2012 2nd International Conference on Consumer Electronics, Communications and Networks (CECNet)*, 687–689, 2012.
6. Zhang, Y., Y. Bi, and S. Wang, "Parameter identification of permanent magnet synchronous motor based on extended Kalman filter and gradient correction," *2020 IEEE International Conference on Mechatronics and Automation (ICMA)*, 718–722, 2020.
7. Wang, Q., G. Zhang, G. Wang, C. Li, and D. Xu, "Offline parameter self-learning method for general-purpose PMSM drives with estimation error compensation," *IEEE Transactions on Power Electronics*, Vol. 34, No. 11, 11103–11115, Nov. 2019.
8. Wang, Q., G. Wang, S. Liu, G. Zhang, and D. Xu, "An inverter-nonlinearity-immune offline inductance identification method for PMSM drives based on equivalent impedance model," *IEEE Transactions on Power Electronics*, Vol. 37, No. 6, 7100–7112, Jun. 2022.
9. Perera, A. and R. Nilsen, "Recursive prediction error gradient-based algorithms and framework to identify PMSM parameters online," *IEEE Transactions on Industry Applications*, Vol. 59, No. 2, 1788–1799, Mar.–Apr. 2023.
10. Ma, X. and C. Bi, "A technology for online parameter identification of permanent magnet synchronous motor," *CES Transactions on Electrical Machines and Systems*, Vol. 4, No. 3, 237–242, Sept. 2020.
11. Sun, P., Q. Ge, B. Zhang, and X. Wang, "Sensorless control technique of PMSM based on RLS on-line parameter identification," *2018 21st International Conference on Electrical Machines and Systems (ICEMS)*, 1670–1673, 2018.
12. She, Z., J. Liu, Q. Liang, and W. Zou, "Identification for PMSM rotor speed based on optimized extended Kalman filter and load torque observer," *2020 IEEE International Conference on Applied Superconductivity and Electromagnetic Devices (ASEMD)*, 1–2, 2020.
13. Li, M., K. Lv, C. Wen, Q. Zhao, X. Zhao, and X. Wang, "Sensorless control of permanent magnet synchronous linear motor based on sliding mode variable structure MRAS flux observation," *Progress In Electromagnetics Research Letters*, Vol. 101, 89–97, 2021.
14. Zhang, J., J. Song, C. Su, J. Hu, and Q. Wang, "Parameter identification of HVDC transmission system model based on intelligent optimization algorithm," *2021 IEEE 11th Annual International Conference on CYBER Technology in Automation, Control, and Intelligent Systems (CYBER)*, 643–647, 2021.
15. Zhang, Z., Z. Chen, S. Liu, and F. Dong, "Parameter identification of Anand constitutive models for SAC305 using the intelligent optimization algorithm," *2019 IEEE 21st Electronics Packaging Technology Conference (EPTC)*, 133–137, 2019.
16. Lv, J., F. Liu, and Y. Ren, "Fuzzy identification of nonlinear dynamic system based on input variable selection and particle swarm optimization parameter optimization," *IEEE Access*, Vol. 8, 220557–220569, 2020.

17. Ortombina, L., D. Pasqualotto, F. Tinazzi, et al., "Magnetic model identification of synchronous motors considering speed and load transients," *IEEE Transactions on Industry Applications*, Vol. 56, No. 5, 4945–4954, 2020.
18. Liu, K. and Z. Q. Zhu, "Position-offset-based parameter estimation using the adaline NN for condition monitoring of permanent-magnet synchronous machines," *IEEE Transactions on Industrial Electronics*, Vol. 62, No. 4, 2372–2383, 2015.
19. Wei, J., Y. Yu, and D. Cai, "Identification of uncertain incommensurate fractional-order chaotic systems using an improved quantum-behaved particle swarm optimization algorithm," *J. Comput. Nonlinear Dyn.*, Vol. 13, No. 5, 1–23, Mar. 2018.
20. Avdeev, A. and O. Osipov, "PMSM identification using genetic algorithm," *2019 26th International Workshop on Electric Drives: Improvement in Efficiency of Electric Drives (IWED)*, 1–4, Moscow, Russia, 2019.
21. Liu, K. and Z. Q. Zhu, "Quantum genetic algorithm-based parameter estimation of PMSM under variable speed control accounting for system identifiability and VSI nonlinearity," *IEEE Transactions on Industrial Electronics*, Vol. 62, No. 4, 2363–2371, 2015.
22. Liu, Z.-H., H.-L. Wei, Q.-C. Zhong, K. Liu, X.-S. Xiao, and L.-H. Wu, "Parameter estimation for VSI-fed PMSM based on a dynamic PSO with learning strategies," *IEEE Transactions on Power Electronics*, Vol. 32, No. 4, 3154–3165, Apr. 2017.
23. Kim, H.-W., M.-J. Youn, K.-Y. Cho, and H.-S. Kim, "Nonlinearity estimation and compensation of PWM VSI for PMSM under resistance and flux linkage uncertainty," *IEEE Transactions on Control Systems Technology*, Vol. 14, No. 4, 589–601, Jul. 2006.
24. Liu, K. and Z. Q. Zhu, "Online estimation of the rotor flux linkage and voltage-source inverter nonlinearity in permanent magnet synchronous machine drives," *IEEE Transactions on Power Electronics*, Vol. 29, No. 1, 418–427, 2013.
25. Liu, Z. H., H. L. Wei, Q. C. Zhong, et al., "Parameter estimation for VSI-fed PMSM based on a dynamic PSO with learning strategies," *IEEE Transactions on Power Electronics*, Vol. 32, No. 4, 3154–3165, 2016.
26. Kim, S. J., H. W. Lee, K. S. Kim, et al., "Torque ripple improvement for interior permanent magnet synchronous motor considering parameters with magnetic saturation," *IEEE Transactions on Magnetics*, Vol. 45, No. 10, 4720–4723, 2009.
27. Accetta, A., F. Alonge, M. Cirrincione, et al., "GA-based off-line parameter estimation of the induction motor model including magnetic saturation and iron losses," *IEEE Open Journal of Industry Applications*, Vol. 1, 135–147, 2020.
28. Wang, M., W. Chang, H. Yang, et al., "Sensorless vector control of permanent magnet synchronous motor based on improved hybrid genetic algorithm," *2019 4th International Conference on Control and Robotics Engineering (ICCRE)*, 21–26, IEEE, 2019.